Preparation of a Sodium Alginate–Poly(vinyl alcohol)–Chitosan Bipolar Membrane and Its Application in the Electrogeneration of Ferrate(VI)

Cai-Xia Xu, Ri-Yao Chen, Xi Zheng, Zhen Chen

College of Chemistry and Materials Science, Experiment Center, Fujian Normal University, Fuzhou 350007, People's Republic of China

Received 3 July 2007; accepted 26 September 2007
DOI 10.1002/app.27396
Published online 26 November 2007 in Wiley InterScience (www.interscience.wiley.com).

ABSTRACT: A sodium alginate (SA)–poly(vinyl alcohol) (PVA)–chitosan (CS) bipolar membrane (BPM) was prepared by a paste method with PVA, SA, and CS as starting materials and modified by Fe^{3+} and GA as a crosslinking agent. The morphology, functional groups, and physical properties of the film were studied by scanning electron microscopy, IR spectroscopy, and tensile testing, respectively. The SA–PVA–CS BPM was used as a separator in the electrolysis cell for electrogenerated ferrate(VI). The results show that the SA–PVA–CS BPM possessed reasonable physical and electrochemical properties. The SA–PVA–CS BPM not only prevented ferrate(VI) from diffusing into the cathode room but also played an important role in the supply of OH^- consumed during the electrogenerated ferrate(VI) process. Compared with the traditional method of preparing ferrate(VI), electrodialysis with the BPM (SA–PVA–CS) had the further advantage of lower alkali and energy consumption. © 2007 Wiley Periodicals, Inc. J Appl Polym Sci 107: 3076–3082, 2008

Key words: crosslinking; ion exchangers; membranes; polyelectrolytes

INTRODUCTION

A bipolar membrane (BPM) is a polymeric layered structure composed of a cation exchange layer and an anion exchange layer. Protons and hydroxide ions are generated by the splitting of water in the interface under a reverse potential bias and migrate to the cathode and anode rooms, respectively.[1,2] Electrodialysis with bipolar membranes (EDBM) is a type of technology that is based on design for the environment and ''green'' chemistry.[3] It has become a new growth point in electrodialysis industries, and great potential exists for it in industry and daily life, such as chemistry production and separation, food processing, biochemical industries, and environmental conservation.[4–7] For instance, Yu et al.[8] reported the recovery of acetic acid from dilute wastewater by means of EDBM. Bazinet et al.[9] developed an electroacidification technology by using EDBM for the food industry. Sidhar[10] successfully synthesized acetoacetic ester using EDBM with methanol splitting, which initiates novel and green paths for organic synthesis.[10] However, there is still no literature concerning electrogenerated ferrate(VI) by EDBM, except by our group.

Ferrate(VI) species is a strong oxidant and has been considered for the treatment of wastewater for years because of its environmentally friendly properties and high efficiency.[11] For instance, it has been used as an efficient water treatment reagent to disinfect microorganisms, partially degrade and oxidize organic and inorganic contaminants, and remove colloidal/suspended particulate materials and heavy metals.[12] Ferrate(VI) can be chemically and electrochemically synthesized, and the electrochemical method has several advantages, such as simple operation, safety, and free hypochlorite. The basic principle of preparing ferrate(VI) salts by the electrolytic method is shown in eqs. (1)–(3). Cast iron is used as the anode and is oxidized to form ferrate(VI) in a highly concentrated OH^- electrolyte. According to eq. (1), for every 1 mol of ferrate(VI) generated in the anode room, 8 mol of OH^- is consumed. This means that a great amount of OH^- is needed during the process of the electrogeneration of ferrate(VI). EDBM technology was used to electrogenerate ferrate(VI) to supply OH^- timely in this study:

$$\text{Anode reaction: } Fe + 8OH^- - 6e^- = FeO_4^{2-} + 4H_2O \quad (1)$$

$$\text{Cathode reaction: } 2H_2O + 2e^- = H_2 + 2OH^- \quad (2)$$

$$\text{Side reaction: } 4OH^- - 4e^- = 2H_2O + O_2 \quad (3)$$

The principle of the electrogeneration of ferrate(VI) with a BPM as the septum is shown in Figure 1. The

Correspondence to: Z. Chen (zc1224@pub1.fz.fj.cn).
Contract grant sponsor: Nature Science Foundations of Fujian Province; contract grant number: DO710009.
Contract grant sponsor: Fujian Development and Evolution Program; contract grant numbers: DH-361 and JH-006.

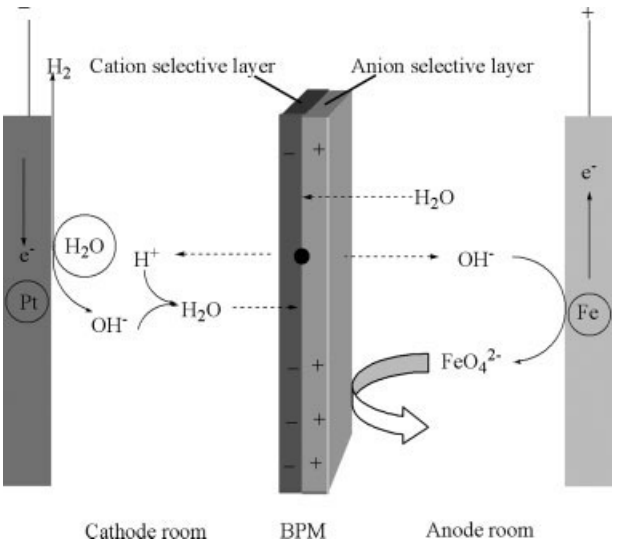

Figure 1 Mechanism of the electrogeneration of FeO_4^{2-} in the electrolysis cell with the BPM as a septum.

generated protons and hydroxide ions by water splitting at the interface of the BPM move to the cathode and anode rooms, respectively. Then, OH^- was guaranteed effectively *in situ* during the electrogeneration of ferrate(VI) in anode room. Meanwhile, ferrate(VI) was prevented from diffusing into the cathode room to be reduced. In our previous work, sodium allyl methyl sulfonate (SAMS)–carboxymethyl cellulose (CMC)–chitosan (CS) BPMs were prepared to electrogenerate ferrate(VI).[13] The route for the preparation of SAMS–CMC–CS BPMs was rather complicated, and the starting material SAMS is not friendly to the environment.

The main objective of this study was to prepare an inexpensive BPM exhibiting a low electrical resistance and reasonably good mechanical properties and to apply the BPM technique to the electrogeneration of ferrate(VI). CS and sodium alginate (SA) as a natural, low-cost polyelectrolyte were expected to be effective materials for the BPM on the basis of their abundance of functional groups, amino groups, and carboxylic groups. SA and CS were blended with poly(vinyl alcohol) (PVA) and modified by Fe^{3+} and glutaraldehyde (GA) as a crosslinking agent, respectively, because PVA possesses serial good properties, such as film-forming abilities, highly hydrophilic natures, excellent mechanics, and good chemical resistance to organic solvents.

EXPERIMENTAL

Materials

CS with an N-deacetylation degree of 90%, SA, PVA-124, GA (25% content in water), and iron trichloride were purchased from Guoyao Chemicals Co., Ltd. (Si Chuan, China). Poly(vinyl sulfate) potassium salt (PVSK), poly(diallyldimethylammonium chloride), and toluidine blue (TB) were all purchased from Wako Pure Chemical Industries Co. Ltd. (Osaka, Japan). Ammonium ferrous sulfate, potassium dichromate, chromium trichloride, and other chemicals (Guoyao Chemicals Co., Ltd., Si Chuan, China) used for the investigations were analytical grade.

Preparation of the SA–PVA–CS BPM

A two-step process was used to prepare the SA–PVA–CS BPM (Fig. 2). A 3 wt % PVA solution was prepared by the dissolution of PVA in distilled water with stirring for 1 h at 90°C; the solution was then kept at 25°C for 24 h. The mixture of 2 wt % SA and 3 wt % PVA solution with a ratio of 3 : 2 was stirred for 2.5 h to make PVA–SA. A crosslinked gelatinous PVA–SA membrane was first cast on a glass plate that was first washed with acid and alkali solutions. Subsequently, it was introduced into a room accompanying solvent evaporation at a controlled rate, and then, the PVA–SA film was immersed in an 8% $FeCl_3$ aqueous solution for 10 min to incorporate a certain concentration of $FeCl_3$ into the membrane. Macroscopically, the membrane appeared light yellow; we refer to this membrane as Fe–PVA–SA.

In the second step, the mixture of 2 wt % CS and 3 wt % PVA solution with the same ratio of 3 : 2 was stirred for 2.5 h with GA as the crosslinking agent; we refer to this mixture as GA–PVA–CS. Then, the GA–PVA–CS solution was cast onto the surface of the Fe–PVA–SA membrane to form the BPM. Finally, this composite membrane was allowed to be totally dried in air at 25°C for around 2 days.

Membrane characterization

Characterization by scanning electron microscopy (SEM) and IR and measurement of the mechanical properties

The morphology of the membranes was examined by SEM (Philips, XL-30, Netherlands Philip Co., Ltd., Netherlands). The characteristic functional groups were investigated by Fourier transform infrared (FTIR) absorption spectroscopy (American Necolet

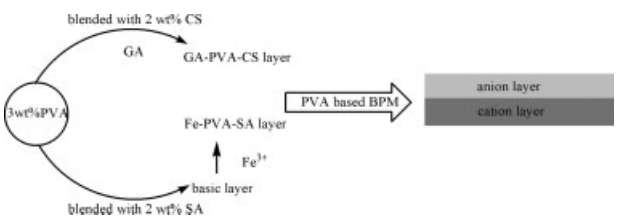

Figure 2 Schematic diagram of the preparation of the SA–PVA–CS BPM.

5700). A Lloyd instrument (Lloyd LR5K, England) was used to determine the mechanical properties of the dry membranes before or after modification. The grip length was 25.00 mm, and the speed of testing was set at a rate of 2.0 mm/min. All the data were given by computer.

Measurement of the current–voltage curves

The current voltage curves of the BPM were conducted in a special design cell similar to the setup employed in a previous study.[14] The cell was conically shape and permitted a large surface for the current electrodes and a small area for the membrane to minimize border effects and make the current through the membrane approximately homogeneous. The BPM, with a cross-section area of 1.04 cm^2, was fixed between the two half-cells. A graphite electrode (2 cm^2) was installed as the working electrode. The current was supplied by a direct-current power system (Instrument and Electrical Equipment Co., Ltd., ZhenJiang, China) (DF1720SB5A). A 0.5*M* Na_2SO_4 electrolyte solution was added to the cell. The volume of each cell was 100 mL. The cell voltages with and without the membrane were measured under the same conditions. The potential differences between both were the actual voltages that appeared across the membrane according to the description by Simons.[15]

Measurement of the swelling degree of the membrane

Before measurement, the membranes were immersed in an alkaline solution for 24 h at room temperature to reach final dilation. Then, the membranes were taken out of the solution and carefully wiped with an absorbent paper before they were weighed (W_s). The weight W_d was obtained for the membrane dried at 80°C in an oven. The degree of swelling (S_w) was determined from the weight difference between the wet and dry membranes according to eq. (4)

$$S_w = (W_s - W_d)/W_d \times 100\% \quad (4)$$

Colloid titration

Colloid titration was carried out for measurement of the charge density of the polyelectrolyte. The concentration of $—NH_3^+$ in the CS polyelectrolyte was measured by titration with PVSK as the counterpolyanion and TB as the metachromatic indicator. As for the measurement of the concentration of $—COO^-$ in the SA polyelectrolyte, 10 mL of poly (diallyldimethylammonium chloride) standard solution was added first; the extra amount of polycation was measured by titration with PVSK and TB as the metachromatic indicator in the same way. The charge density of the polyelectrolyte was calculated by the following equations:

$$\mathrm{ED}_{(\mathrm{CS})} = \frac{C \times V}{1000 \times m} \quad (5)$$

$$\mathrm{ED}_{(\mathrm{SA})} = \frac{C \times (10 - V)}{1000 \times m} \quad (6)$$

where ED is the charge density (mmol/g), V is the consumed volume of the PVSK standard solution (mL), C is the concentration of PVSK standard solution (1.0 mmol/L), and m is the weight of the polyelectrolyte.

Apparatus for the electrochemical generation of ferrate(VI)

The electrogeneration of ferrate(VI) was carried out with a laboratory-scale electrolysis cell, which was composed of one cathode room and one anode room separated by the SA–PVA–CS BPM, as shown in Figure 1. Gray cast iron (Q235 C% ≈ 0.2%) and platinum were installed as the anode and cathode electrodes, respectively. The effective area of the gray cast iron was 15.6 cm^2. In both chambers were added 110 mL of 14 mol/L NaOH. A constant current was applied by a direct-current source (DF1720SB5A). The concentration of ferrate(VI) was determined by chromite every 15 min.[16]

RESULTS AND DISCUSSION

SEM analysis

The microscopic analyses of the SA–PVA–CS membrane are shown in Figure 3. As expect, a two-layer structure was observed [Fig. 3(c)]. Both layers had a dense surface without pores. The upper layer (GA–PVA–CS) was more compatible with a homogeneous surface [Fig. 3(a)], whereas the bottom layer (Fe–PVA–SA) had a close-net structure [Fig. 3(b)]. The distinct microcosmic phase of the two layers was attributed to the different composition and the cross-linkage.

FTIR spectra

Figure 4 displays the FTIR spectra of the PVA, CS, GA–PVA–CS, Fe–PVA–SA, and SA membranes. The FTIR spectrum of the pure PVA membrane showed absorption peaks at about 3296 cm^{-1} for —OH and about 1419 and 1091 cm^{-1} for the —C—O group. The spectrum of CS exhibited characteristic IR peaks of $—NH_2$ at 1551 cm^{-1} and of $—NHCOCH_3$ at 1635 cm^{-1}. Figure 4(c) illustrates that the effect of GA on the chemical structure of the PVA–CS membrane. Broadened absorption peaks for the —OH

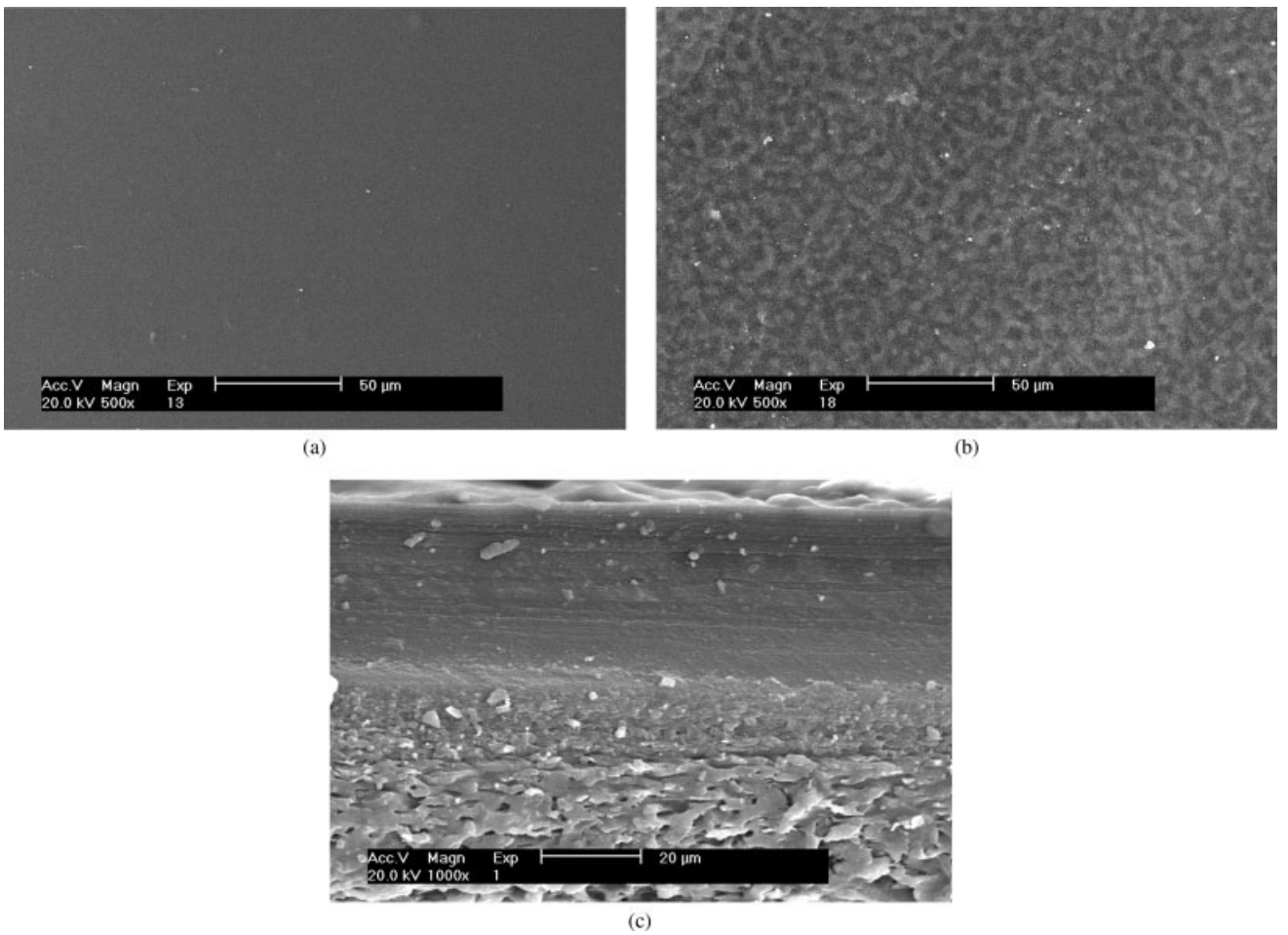

Figure 3 SEM micrographs of the SA–PVA–CS BPM: (a) GA–PVA–CS layer, (b) Fe–PVA–SA layer, and (c) cross section of SA–PVA–CS.

group in PVA were found. The specific change was due to the reaction between hydroxyl groups and GA. The absorption of the $—NH_2$ group was decreased because of the reaction between GA and the $—NH_2$ group to form a —N=C bond.[17,18] The reaction in hydroxyl groups, amido, and GA was considered evidence of compatibility between PVA and CS [Fig. 3(a)].

The characteristic absorption peaks of the $—COO^-$ functional group appeared at 1590 and 1414 cm^{-1}. When we compared SA with the Fe–PVA–SA membrane, a weaker absorption peak of $—COO^-$ was observed in Fe–PVA–SA; this meant that SA and PVA were modified by Fe^{3+} to form a cross-net structure, which was in agreement with the SEM results [Fig. 3(b)]. Thus, Fe^{3+} as a center cation was coordinated to $—COO^-$ in the Fe–PVA–SA chelate polymer.[19,20]

Properties of the monolayer

The charge densities of CS and SA were about 5.57 and 3.78 mmol/g, respectively. Compared with values in the literatures, such as 0.76 mmol/g for $—NH_3^+$ and 0.33 mmol/g for $—COO^-$ in carboxymethyl CS,[21] and 0.162, 0.176, and 0.189 mmol/g for $—NH_3^+$ in cationic starches,[22] CS and SA possessed higher charge densities. The basic properties of the

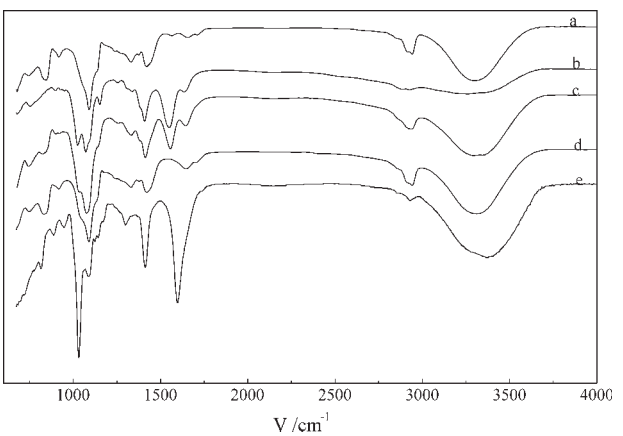

Figure 4 IR spectra of (a) PVA, (b) CS, (c) GA–PVA–CS, (d) Fe–PVA–SA, and (e) SA membranes.

TABLE I
Characteristics of the GA–PVA–CS and Fe–PVA–SA Membranes

Membrane	Ion exchange capacity (mequiv/g dry)	Water content (%)	Functional groups
GA–PVA–CS	1.86	48.74	$-NH_2$, $-N{=}CHR$, $-NHCOCH_3$
Fe–PVA–SA	2.24	46.51	$-COO^-$

GA–PVA–CS and Fe–PVA–SA membranes are listed in Table I.

The mechanical capabilities of the membranes before and after modification are shown in Table II. Because of the ring structure in the polymer main chain and the intermolecular hydrogen bond in the polar groups (—OH, $-COO^-$, and $-NH_2$) present in the polymer, SA and CS were ascribed with a rigid structure with a relative high Young's modulus (1217.3 and 907.1 MPa, respectively). The flexibility of Fe–PVA–SA and GA–PVA–CS obviously increased with decreasing Young's modulus (297.5 and 214.1 MPa, respectively) and rising elongation at break when compared to the CS and SA membranes. Hence, the degree of rigidity obviously decreased. In general, the plastic material had a higher tensile strength, whereas the rigid material was more pressure-proof. Thus, the breaking strain dropped a little. The results indicated that the mechanical properties were effectively because of the formation of the close-net crosslinking structure after modification.

Swelling degree of the SA–PVA–CS membrane

Because the electrochemical generation of ferrate(VI) reaction had to be set up in an alkaline solution [eq. (1)], the swelling of SA–PVA–CS in different concentrations of OH^- solution was studied. As shown in Figure 5, the swelling of the SA–PVA–CS membrane underwent dramatic changes after crosslinking, although SA and CS are well known as soluble polymers. The swelling degree of the SA–PVA–CS membrane increased significantly at the lower OH^- concentration (<10 mol/L) and then decreased with increasing OH^- concentration (10–14 mol/L). This tendency of the swelling degree was quite similar to that of the carboxymethyl CS membrane in alcoholic solution and is explained by the theory of plasticization.[23] A certain concentration of OH^- acted as a plasticizer for the SA–PVA–CS membrane.

In fact, the swelling of the BPM affected the electrochemical properties of the BPM in the electrolysis bath. Sufficient water had to be kept in the BPM to make the system functional because water molecules in the BPM were split into H^+ and OH^- by the electric field during the electrolysis. In the system of the electrochemical generation of ferrate(VI), the swelling of SA–PVA–CS ($\approx$ 35%) would help the BPM to maintain better shape stability and mechanical strength as well as sufficient water flux into the interface region to replenish the consumed water.

Permeability of OH^-

As described previously, the $-NHCOCH_3$, $-NH_2$ weak basic group in the SA–PVA–CS BPM enhanced the dissociation of the water, according to Simons' theory.[24] Considering the alkaline condition for the generation of ferrate(VI) and the OH^- exchange ability of the anion layer (GA–PVA–CS), we investigated the concentration of OH^- in the anode room using the SA–PVA–CS BPM and the GA–PVA–CS membrane as a septum, respectively. Figure 6 plots the concentration of OH^- increasing with time at 2 mA/cm^2. For the SA–PVA–CS BPM, OH^- dissociated from water at the interface directly migrated into the anode room. Thus, in the same electrolysis conditions, the concentration of OH^- in the anode room with SA–PVA–CS BPM as a septum was greater than that of the corresponding monolayer (GA–PVA–CS). SA–PVA–CS BPM was available to generate ferrate(VI) because of the sufficient supplement of OH^-. Another advantage was that the electrolyte

TABLE II
Mechanical Capabilities of the Membranes Before and After Modification

Membrane	Rigidity (N/m)	Young's modulus (MPa)	Breaking strain (MPa)	Elongation at break (%)
CS	22,134	907.1	12.6	67.9
GA–PVA–CS	5,482	214.1	8.9	47.9
SA	20,938	1217.3	10.5	17.6
Fe–PVA–SA	11,320	297.5	9.2	40.0

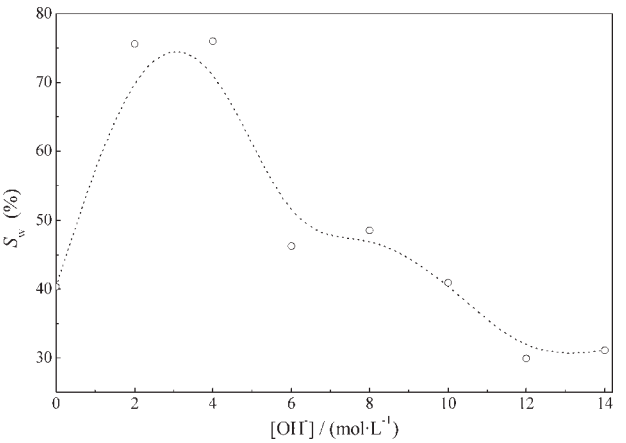

Figure 5 Effect of OH^- on the swelling capacity.

solution could be maintained as a strong base, which prevented the reduction of ferrate(VI).

Electrochemical generation of ferrate(VI)

As shown in Figure 7(a), the concentration of the electrochemical generation of ferrate(VI) increased as time passed. When current passed across the BPM, electrical conduction was achieved by the transportation of H^+ and OH^- ions generated by the electrodissociation of water in the BPM. The higher the current density was, the more OH^- was generated. The net results were that an alkaline solution was formed in the anode room on the anion-exchange side of the BPM, where ferrate(VI) was subsequently generated. The anion-exchange layer could be rationalized in terms of minimizing concentration polarization and membrane fouling by electrostatic repulsion to ferrate from its surface. SA–PVA–CS improved the ionic conductivity and prevented ferrate(VI) from diffusing into the cathode room. The concentration

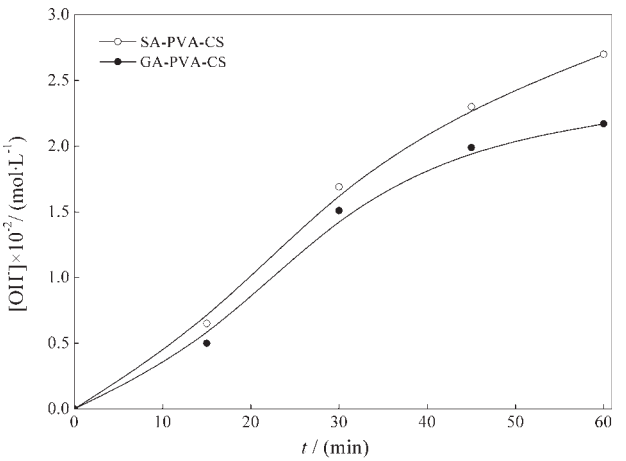

Figure 6 Changes in the concentration of OH^- in the anode chamber.

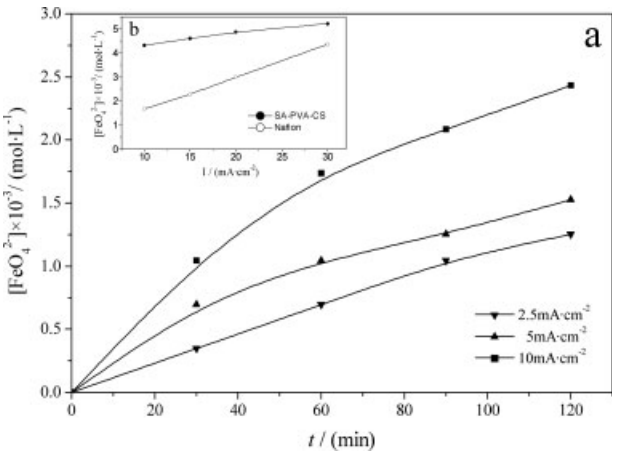

Figure 7 (a) Dependence of the FeO_4^{2-} concentration on the duration of electrolysis and (b) comparison of Nafion and the SA–PVA–CS BPM for 2.5 h of electrolysis.

of ferrate(VI) was about 2.43 mmol/L at 10 mA/cm^2 for 2 h.

A comparison of the electrogeneration of ferrate(VI) by the SA–PVA–CS BPM with a Nafion membrane under the same operating conditions is shown in Figure 7(b). The concentration of ferrate(VI) generated by the SA–PVA–CS BPM was obviously higher than that by the Nafion membrane as septum at different current densities after 2.5 h of electrodialysis.

In our study, Fe^{3+} was immobilized in the cation-exchange layer. Hanada et al.[25] suggested that the cation-exchange layer, which was pretreated by heavy-metal ions such as Fe^{2+}, Fe^{3+}, Ti^{4+}, Sn^{2+}, Sn^{4+}, Zr^{4+}, Pd^{2+}, and Ru^{3+}, would reduce the voltage of electrolysis. This effect might have been due to a special structure of the transition region after the heavy metal ions penetrated into the junction of the BPM, which might have resulted in a more hydrophilic interphase and consequently accelerated the water dissociation. The voltage of the electrolysis bath was about 2.1 V during the electrogeneration of

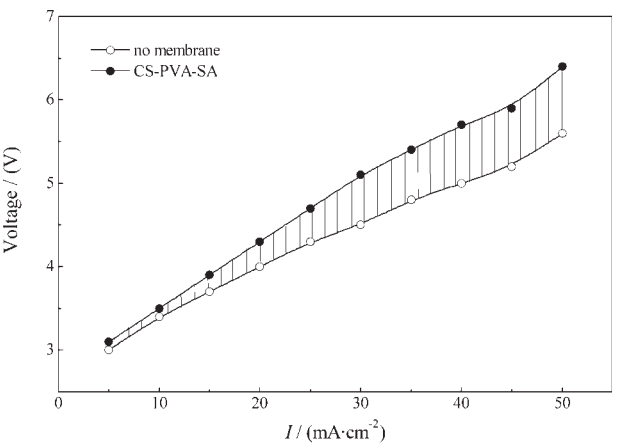

Figure 8 Current voltage curve of the SA–PVA–CS BPM. *I*, current density.

ferrate(VI) at 10 mA/cm^2. The electrical energy consumption was lower.

The potential differences equipped with and without membranes indicated the IR drop of the membrane, shown in Figure 8. However, the IR drop of the membrane increased with increasing current density, which was as low as 0.2 V at 10 mA/cm^2, in agreement with the literature.[14]

CONCLUSIONS

Natural, low-cost polysaccharides (CS and SA) were successfully modified by blending with PVA with $FeCl_3$ and GA as crosslinkages. The SA–PVA–CS BPM was prepared by a two-step method and was composed of a Fe–PVA–SA cation layer and a GA–PVA–CS anion layer. It was used as the separator in the electrolysis cell for electrogenerated ferrate(VI). The OH^- consumed in the generation of ferrate(VI) was effectively supplied when the proton (H^+) and hydroxide (OH^-) ions generated by the spitting of water migrated to the anode and cathode, respectively. Therefore, the SA–PVA–CS BPM holds promise for application in the electrogeneration of ferrate(VI) for lower energy consumption.

References

1. Chilcott, T. C.; Coster, H. G. L.; George, E. P. J Membr Sci 1995, 108, 185.
2. Simons, R. J Membr Sci 1993, 78, 13.
3. Huang, C. H.; Xu, T. W. Environ Sci Technol 2006, 40, 5233.
4. Xu, T. W. Resour Conserv Recy 2002, 37, 1.
5. Ferrer, J. S. J.; Laborie, S.; Durand, G.; Rakib, M. J Membr Sci 2006, 280, 509.
6. Cherif, A. T.; Molenat, J.; Elmidaoui, A. J Appl Electrochem 1997, 27, 1069.
7. Xu, T. W. J Membr Sci 2005, 263, 1.
8. Yu, L. X.; Guo, Q. F.; Hao, J. H.; Jiang, W. J. Desalination 2000, 129, 283.
9. Bazinet, L.; Lamarche, F.; Ippersiel, D. Trends Food Sci Tech 1998, 9, 107.
10. Sridhar, S. J Membr Sci 1996, 113, 73.
11. Jiang, J. Q.; Wang, S.; Panagoulopoulos, A. Desalination 2007, 210, 266.
12. Jiang, J. Q.; Lloyd, B. Water Res 2002, 36, 1397.
13. Ren, Y. X.; Chen, Z.; Chen, R. Y.; Zheng, X.; Geng, Y. M. Cent Eur J Chem 2007, 5, 177.
14. Xu, T. W.; Yang, W. H. J Membr Sci 2004, 238, 123.
15. Simons, R. Electrochim Acta 1986, 31, 1175.
16. Schreyer, J. M.; Thompson, G. W.; Ockerman, L. T. Anal Chem 1950, 22, 1426.
17. Yang, J. M.; Su, W. Y.; Leu, T. L.; Yang, M. C. J Membr Sci 2004, 236, 39.
18. Yeom, C. K.; Lee, K. H. J Membr Sci 1996, 109, 257.
19. Abd-El-Aziz, A. S.; Carraher, C. E.; Pittman, C. U.; Sheats, J. E.; Zeldin, M. Macromolecules Containing Metal and Metal-Like Elements. Volume 1. A Half-Century of Metal- and Metalloid-Containing Polymers; Wiley: Hoboken, NJ, 2003.
20. Rao, P. S.; Krishnaiah, A.; Smitha, B.; Sridhar, S. Sep Sci Technol 2006, 41, 979.
21. Wu, Z. H.; Chen, S. P. Fine Chem 2001, 18, 98.
22. Wu, Z. H.; Chen, S. P. J Anal Sci 2001, 78, 207.
23. Lee, Y. M.; Shin, E. M.; Noh, S. T. Angew Makromol Chem 1991, 192, 169.
24. Simons, R. Nature 1979, 280, 824.
25. Hanada, F.; Hirayama, K.; Ohmura, N.; Tanaka, S. U.S. Pat. 5, 221,455 (1993).